7.6 The results of the laboratory hot rolling process on the YS/UTS ratio

The five alloys #1 to #5 were hot rolled with the same pass numbers, pass strains, pass strain rates and the same total strain in rough and finish rolling on a laboratory mill while the same reheating conditions of 1225 ºC for 60 min were also used. The first rough rolling temperature and the finish rolling temperature, respectively, were very similar for all five experimental alloys. The accelerated cooling rate after finish rolling was also the same at about 47 ºCs^{-1}, for all five experimental alloys, and was 39 ºCs^{-1} for the Mittal steel alloy #6. The simulated coiling after cooling was at a temperature of 600 ºC for 24 hrs. The detailed variables in the hot rolling process for alloys #1 are listed in tables 7.7.

Table 7.7 The laboratory hot rolling parameters for alloy #1

Pass No.		R1	R2	reheating	R3	R4	R5	F1	reheating	F2	reheating	F3
Tempera-ture (ºC)	in	1190	1060	1225 5 min	1140	1070	1020	910	930 5 min	890	930 5 min	890
	out											860
t_{ip} (s)		23	--		16	14	16	--		--		--
Gauge (mm)	in	43	37		28	20	13.6	10.3		8.3		6.9
	out	37	28		20	13.6	10.3	8.3		6.9		6
Pass ε		0.15	0.28		0.34	0.38	0.28	0.22		0.18		0.14
Total ε		1.43						0.54				
Reduction(%)		76						42				
$\dot{\varepsilon}$ (s^{-1})		1.67	2.43		3.15	3.92	4.00	4.07		4.00		3.89

N.B.: The R and F in the table stand for roughing and finishing passes, respectively.

The precise details for the other five alloys #2 to #6, which were very similar to those of alloy #1, are shown in Appendix A. Sample #M1-11 of alloy #6 was taken as a reference to study the microstructures and carry out TEM work.

As can be seen in the table above, the pass strain in the rough rolling stage is more than 0.2 (except for the first pass) in order to obtain a fine recrystallised austenite grain size. The heavy total reduction for alloys #1 to #5, i.e. 76% in rough rolling, 42% in finish rolling and 86% in total, contributes to an optimum combination of strength and toughness through a fine size. Rapid cooling of 47 ºCs^{-1} is useful for the

formation of an acicular ferrite microstructure. The alloy #6 was also used to study the effect of cooling rate, coiling temperature and deformation vis-à-vis the ratio of yield strength to ultimate tensile strength (see Appendix H).

7.7 Volume fraction of acicular ferrite

The volume fraction of acicular ferrite was measured by image-analysis software on shadowed carbon extraction replicas from TEM micrographs taken at 980 times magnification on the experimental alloys #1 to #5. The results are shown in table 7.8 below. Alloy #1 is similar to the Mo-free reference alloy #6 in chemical composition, whereas alloys #2 to #5 contained varying amounts of molybdenum.

Table 7.8 Measured results of volume fraction of acicular ferrite

Alloy #	#1	#2	#3	#4	#5
Molybdenum (%wt)	0.01	0.09	0.09	0.12	0.22
Volume fraction of AF (%)	55.4	46.3	49.4	52.0	46.8
Volume fraction of PF (%)	44.6	53.7	50.6	48.0	53.2

NB. AF-acicular ferrite and PF-polygonal ferrite

Although there appears to be a small effect of molybdenum in affecting the volume fractions of AF and PF, the effect is relatively small and probably needs further study to confirm this.

7.8 Mechanical properties

7.8.1 Results of experimental alloys

The mechanical properties of the five experimental alloys that were hot rolled in the laboratory mill (see section 7.6 above) are given in table 7.9 and the individual curves of strength versus elongation are shown in Appendix G. The longitudinal and transverse (to the rolling direction) values in the table were the average of five samples per direction per alloy except for only four samples for alloy #5 (both directions) and the transverse direction only for alloy #1. The yield strength was taken as the proof strength at 0.5% permanent strain for continuous yielding.

Table 7.9 Mechanical properties of the experimental alloys

Alloy #	Sample direction	YS, MPa	UTS, MPa	YS/UTS	Elongation (%)	Yield type
1	Longitudinal	463	555	0.83	33	D
	Transverse	454	547	0.83	31	D
2	Longitudinal	504	589	0.86	33	D
	Transverse	478	591	0.81	27	D
3	Longitudinal	467	558	0.84	36	D
	Transverse	470	558	0.84	30	D
4	Longitudinal	472	559	0.84	33	D
	Transverse	494	581	0.85	30	D
5	Longitudinal	492	573	0.86	33	D
	Transverse	500	592	0.84	27	C
API specification[12]	X65	≥448	≥530	≤0.93	≥20.5	
	X70	≥482	≥565	≤0.93	≥19	
	X80	≥551	≥620	≤0.93	≥17.5	

NB. YS-yield strength, UTS-ultimate tensile strength, D-discontinuous, C-continuous

7.8.2 Results of mechanical properties for different cooling rates, coiling temperatures and deformation values

7.8.2.1 Effect of cooling rate with no coiling and no prior deformation

The mechanical properties are shown in tables 7.10 and 7.11 for samples subjected to a series of cooling rates after austenitisation and with no prior deformation and no simulated coiling process. Controlled cooling was done by means of helium gas cooling on the Gleeble testing machine at zero load and with conditions of no deformation. The curves of strength versus elongation are shown in Appendix B and C for alloys #6 and #3, respectively.

Table 7.10 Mechanical properties of samples #A124 of the Mo-free alloy #6 with no coiling and no prior deformation

Cooling rate ($^oCs^{-1}$)	YS, MPa	UTS, MPa	YS/UTS	Yield type
1	439	573	0.77	C
5	461	587	0.78	C
10	491	613	0.80	C
21	551	663	0.83	C
40	603	732	0.82	C
51	648	763	0.85	C

Table 7.11 Mechanical properties of samples #AF3F of alloy #3 (with 0.09% Mo) and with no coiling and no prior deformation

Cooling rate ($^oCs^{-1}$)	YS, MPa	UTS, MPa	YS/UTS	Yield type
1	475	593	0.80	C
5	483	579	0.83	C
10	508	606	0.84	C
20	534	625	0.85	C
40	542	640	0.85	C
54	547	648	0.84	C

7.8.2.2 Effect of cooling rate with coiling but without deformation

Results are given in tables 7.12 and 7.13 for the Mo-free alloy #6 treated similarly as above after austenitisation and without prior deformation but with various cooling rates and with subsequent coiling simulations at 600 (sample #A113) and 575 ºC (sample #B113). The individual curves of strength versus elongation are shown in Appendix D and E for 600 and 575 ºC coiling, respectively.

Table 7.12 Mechanical properties of samples #A113 of the Mo-free alloy #6 with 60 min coiling at 600 ºC without prior deformation

Cooling rate (ºCs^{-1})	YS, MPa	UTS, MPa	YS/UTS	Yield type
1	494	635	0.78	C
5	478	619	0.77	C
10	492	650	0.76	C
20	502	650	0.77	C
40	500	651	0.77	C
60	500	646	0.77	C

Table 7.13 Mechanical properties of samples #B113 of alloy #6 with 60 min coiling at 575 ºC without prior deformation

Cooling rate (ºCs^{-1})	YS, MPa	UTS, MPa	YS/UTS	Yield type
1	435	566	0.77	C
5	518	647	0.80	C
10	502	643	0.78	C
20	477	638	0.75	C
40	503	651	0.77	C
60	484	638	0.76	C

7.8.2.3 Effect of cooling rate with 575 ºC coiling and a 33% prior reduction below the T_{nr}

Table 7.14 shows the mechanical properties of the Mo-free alloy #6 with a 575 ºC coiling simulation and a 45% prior reduction in total but 33% reduction below the T_{nr} while the curves of strength versus elongation are shown in Appendix F.

Table 7.14 Mechanical properties of samples #TEN06 for the Mo-free alloy #6 with 60 min coiling at 575 ºC and a 33% prior reduction below the T_{nr}

Cooling rate (ºCs^{-1})	YS, MPa	UTS, MPa	YS/UTS	Yield type
1	434	536	0.81	D
5	528	626	0.84	D
10	514	605	0.85	D
19	568	664	0.86	D
34	528	639	0.83	D

7.9 Transformed microstructures of the alloys

7.9.1 Optical micrographs

The optical microstructures of the five experimental alloys after a rapid cooling rate of 47 ºCs^{-1} and the reference alloy #6, are shown in figures 7.29.

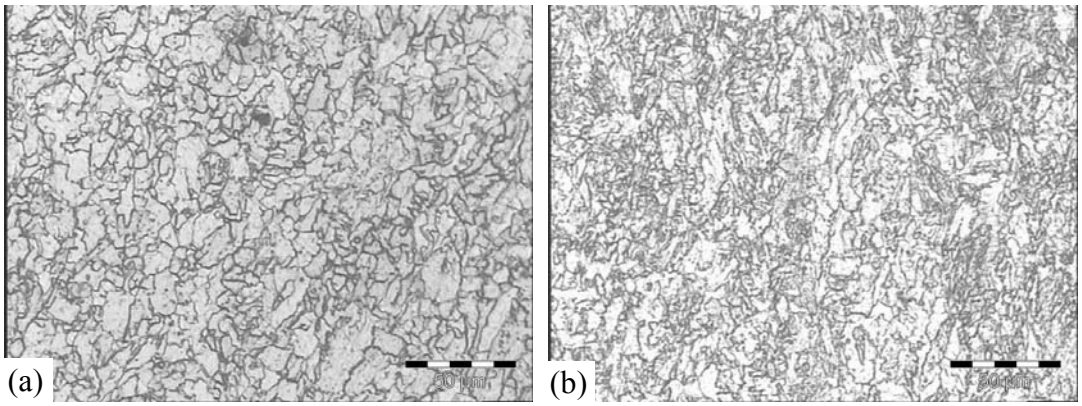

(a) (b)

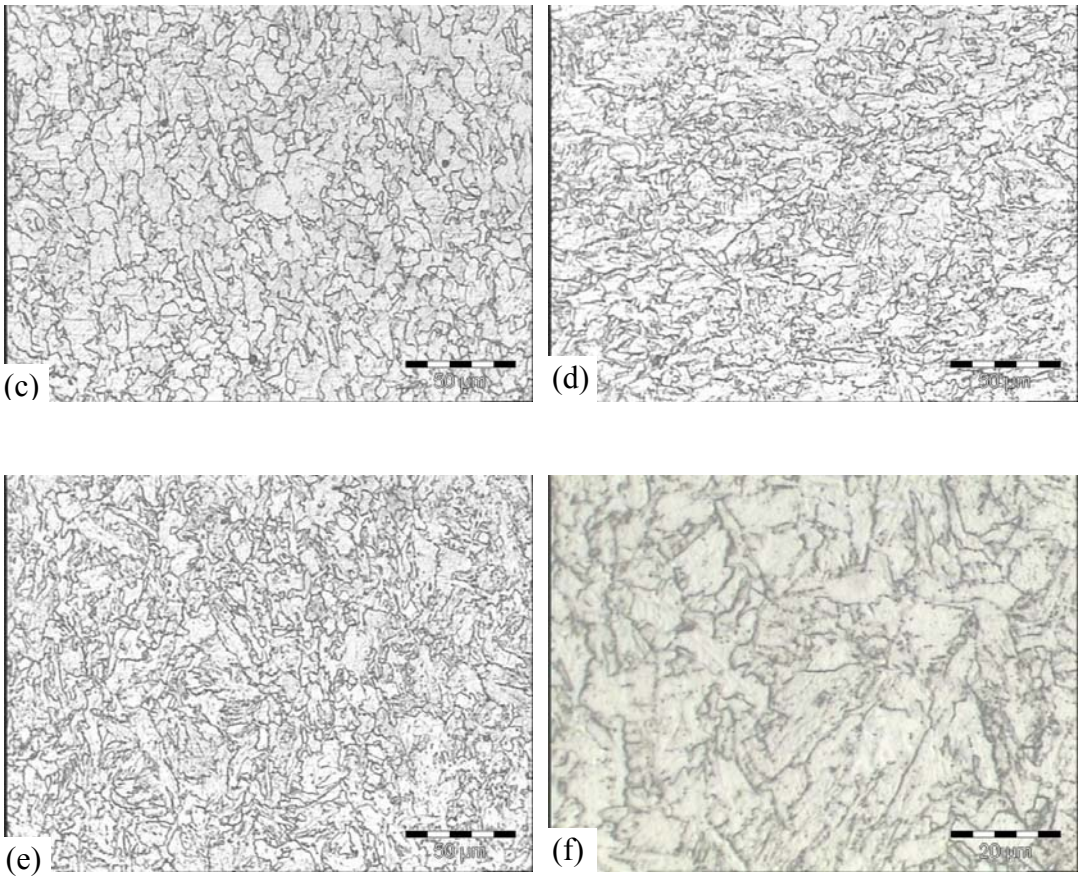

Figure 7.29 The optical microstructure, etched in a 2% Nital solution for 5 seconds, after a rapid cooling rate of 47 ºCs^{-1} for the experimental alloys (a) #1, (b) #2, (c) #3, (d) #4, (e) #5 and, (f) the reference Mo-free alloy #6 cooled at a rate of 39 ºCs^{-1}.

As may be seen in figure 7.29, the optical microstructures for all five experimental alloys #1 to #5 in the as-rolled condition, are similar. They appear to be typical of acicular ferrite, consisting of a "white" phase and an irregular "grey" phase with no clearly etched grain boundaries in the microstructure. In a low carbon low alloyed steel when etched with 2% Nital, polygonal ferrite usually appears as a white coloured phase. From figure 7.29, it is uncertain, however, to establish without any doubt the presence of polygonal ferrite or whether the microstructure shows a 100% acicular ferrite or a mixture of both acicular ferrite and polygonal ferrite. If the polygonal ferrite is mixed within the acicular ferrite structure, it can not be recognised with any confidence. The microstructure of reference alloy #6 consists of a similar microstructure as the five experimental alloys. Accordingly, it was necessary to confirm by other means whether any polygonal ferrite exists in these microstructures.

7.9.2 Microstructures examined by SEM

The Scanning Electron Microscopy (SEM) (Model JEOL JSM-5800LV) was used first in an attempt to identify the presence of polygonal ferrite in the microstructure. The SEM microstructures for the experimental alloys etched in a 2% Nital, are illustrated in figure 7.30 below.

It seemed that there were two different types of microstructures or matrix phases, one is raised above the mean level of the etched plane (marked in "A"), while the other is sunken below this mean plane (marked in "B"). No fine details within each matrix phase can be seen, however, and the SEM was, therefore, not the final answer as to identify the phases which were present.

Next, high resolution SEM (Model JEOL JSM-6000F) micrographs were taken after varying the etching time from 10 to 120 seconds in an attempt to identify these two phases. Figure 7.31 represents the structures of the as-rolled experimental alloys under high resolution SEM after only 5 seconds etching. The microstructures appear relatively similar to those in figure 7.30 although the differences in etching depth between the "raised" and the "sunken" matrix were accentuated. The SEM micrographs after various etching times ranging from 10 to 120 seconds, are shown in figure 7.32. Although the differences in etching depth between the two types of matrix areas are once more, evident, the lack of any finer details of the internal structure within each of the two types of matrix areas did not assist in identifying them conclusively (although one may be tempted to conclude that the deeper etched matrix areas could possibly be acicular ferrite due to its higher dislocation content while the lesser etched matrix areas could possibly be polygonal ferrite with a lower dislocation content). Accordingly, high resolution SEM analysis was also found not to be a totally satisfactory technique to fully identify the matrix microstructures in the present alloys.

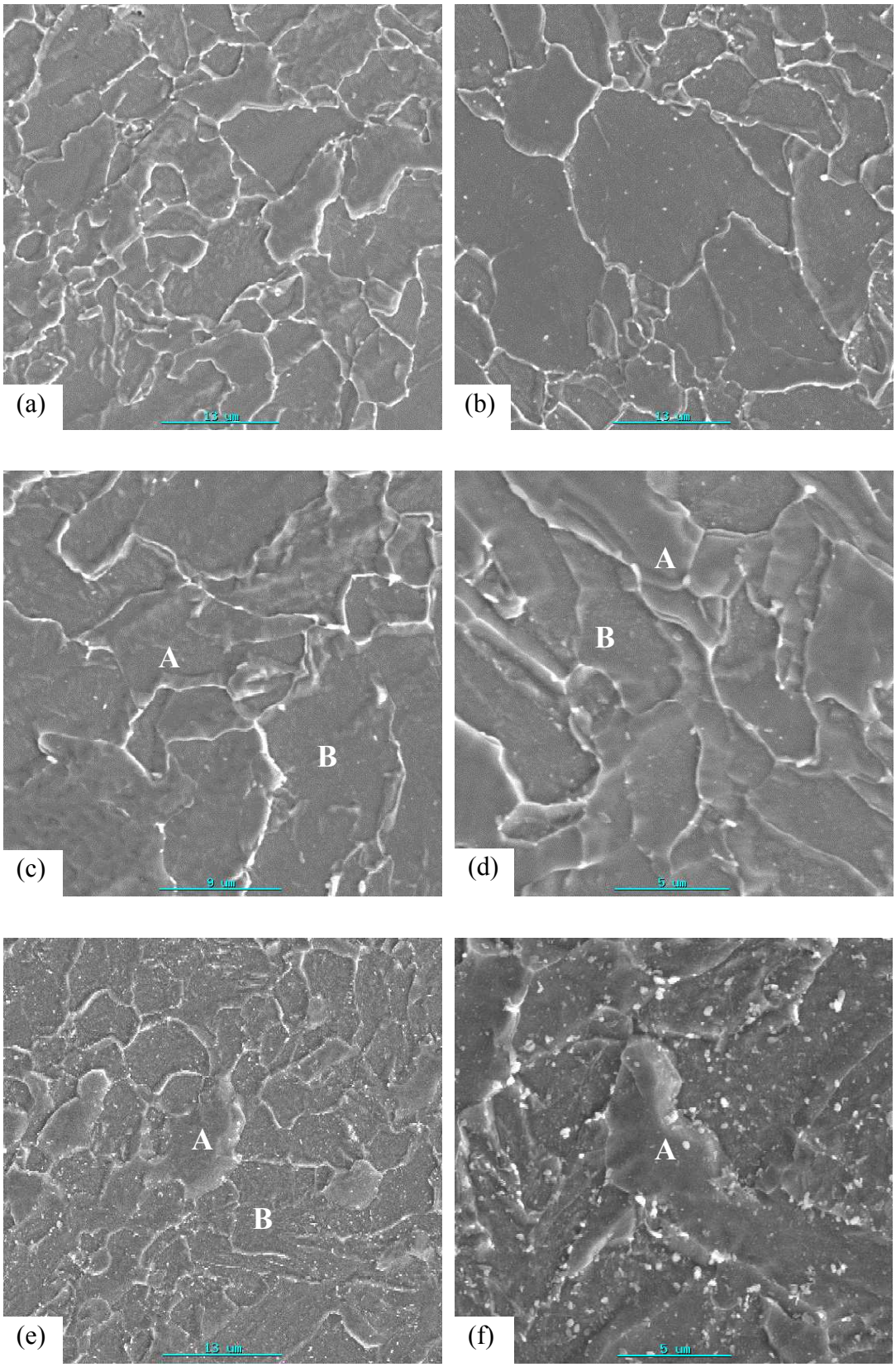

Figure 7.30 The SEM micrographs after a rapid cooling rate of 47 ºCs^{-1}(etched in 2% Nital for 5 seconds) for the experimental alloys (a) #1, (c) #2, (c) #3, (d) #4, (e) #5 and, (f) the reference alloy #6 cooled at a rat of 39 ºCs^{-1}.

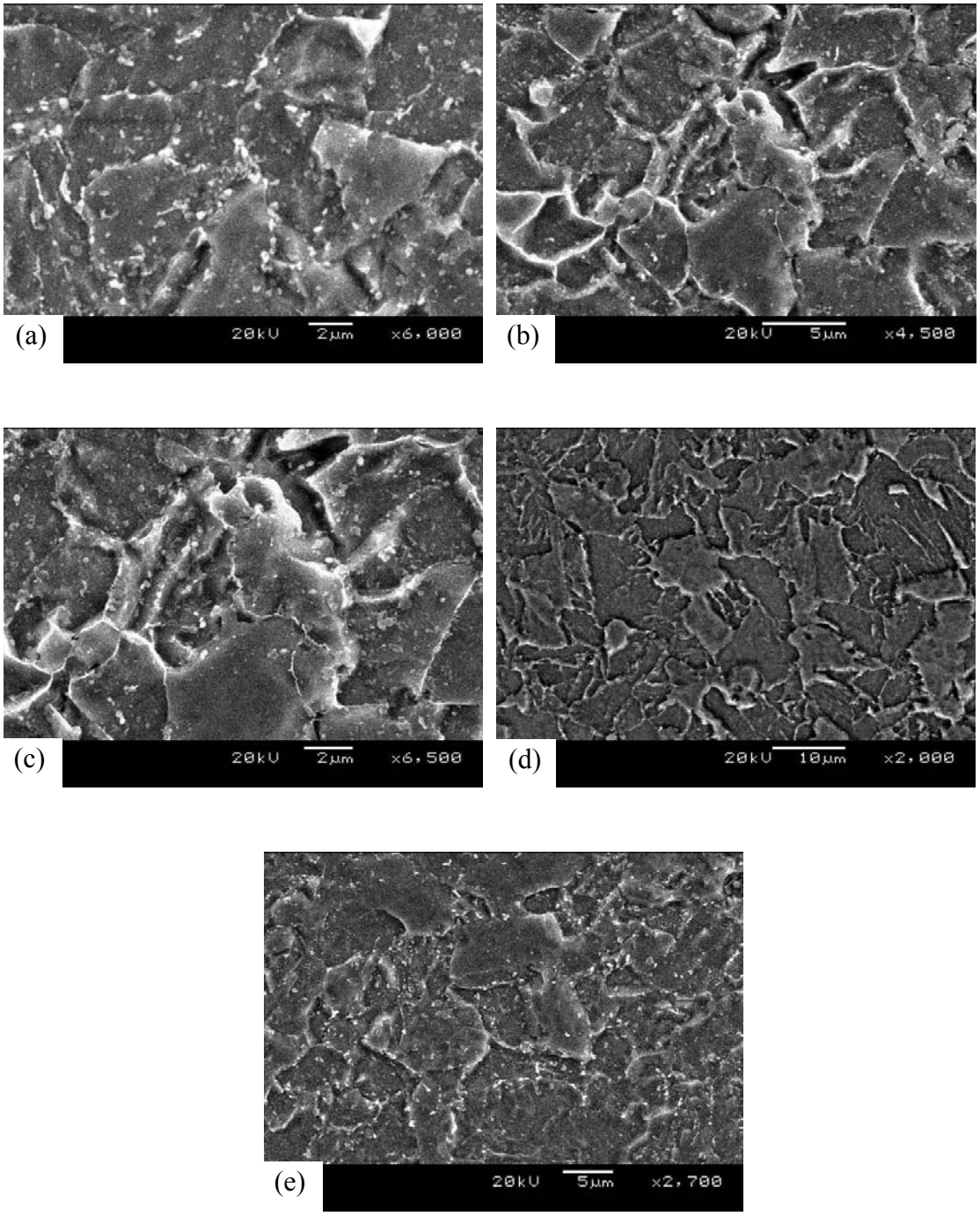

Figure 7.31 The micrographs in the as-rolled condition by high resolution SEM after a rapid cooling rate of 47 ºCs^{-1}(etched in 2% Nital for 5 seconds) for the experimental alloys (a) #1, (c) #2, (c) #3, (d) #4 and, (e) #5.

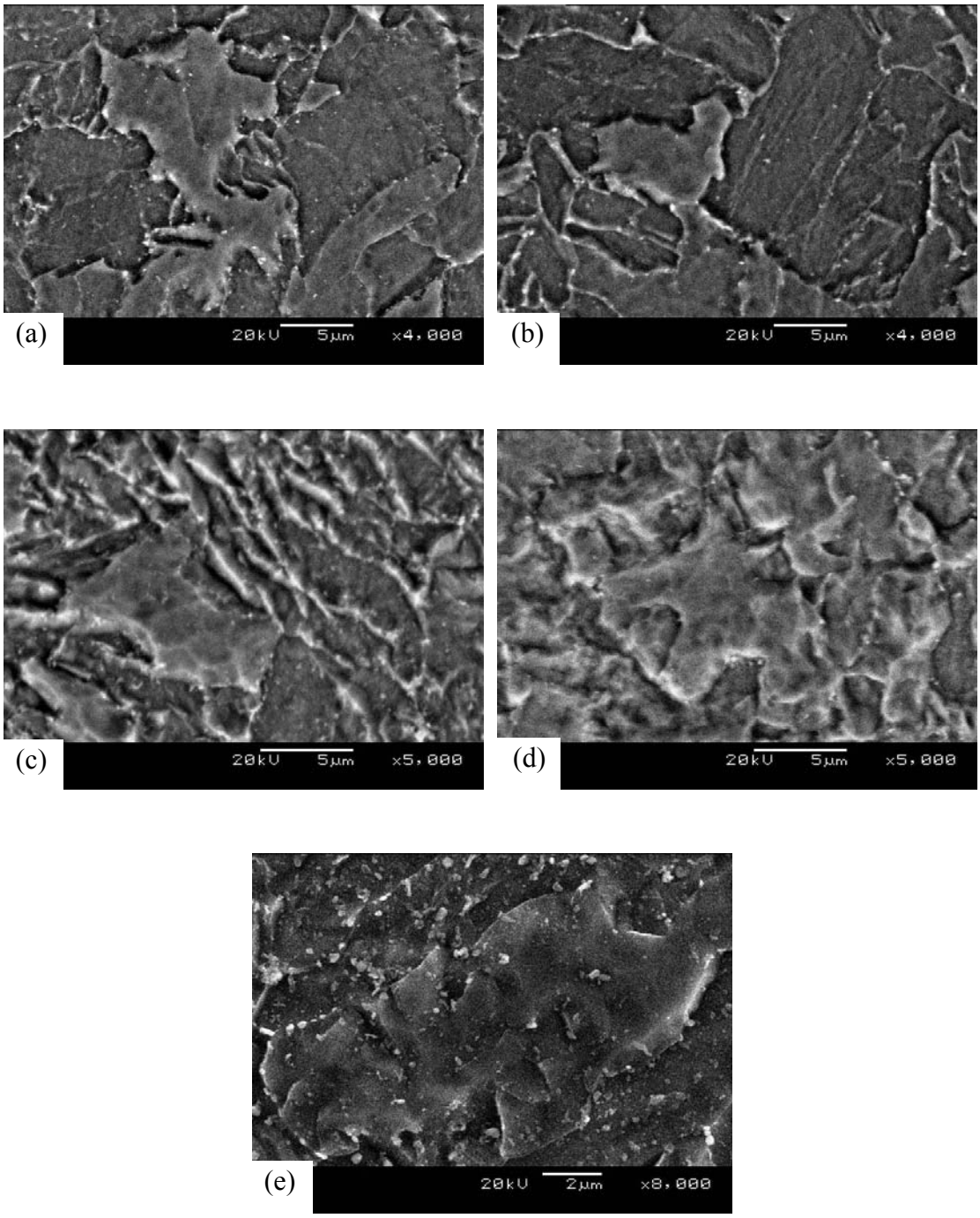

Figure 7.32 The high resolution SEM micrographs in the as-rolled condition after a rapid cooling rate of 47 ºCs^{-1} for the experimental alloy #1 etched in 2% Nital for (a) 10seconds, (c) 15 seconds, (c) 30 seconds, (d) 60 seconds and, (e) 120 seconds.

7.9.3 TEM studies of acicular ferrite on carbon replicas

Carbon extraction replicas with or without Au-Pd shadowing and thin foils were finally used to identify any differences between the matrix phases of acicular ferrite and polygonal ferrite. An etching time from 30 to 60 seconds in a 2% Nital solution was used to obtain a relief on the etched surface on the specimens. A deeply etched relief surface before they are carbon coated, enhances the shadowing of samples.

The TEM micrograph of an unshadowed carbon extraction replica for alloy #6 (reference alloy and Mo-free) is shown in figure 7.33. It appears once more that there are two different matrix phases in the as-rolled reference alloy #6. The quality of the image is a little better than that of the SEM micrographs in figures 7.30 and 7.32. Hence it seemed that carbon extraction replicas may be an improved technique to reveal the finer details of these matrix phases in the alloys, particularly if shadowing by Au-Pd is used before applying the carbon coating to accentuate the relief on the etched surface. Figure 7.34 shows such a shadowed microstructures of alloy #6.

Figure 7.34 shows the marked improvement introduced by shadowing if compared to the unshadowed case in figure 7.33 on the same alloy. The “raised” matrix area (note the direction of the shadow at its edge which is the same as that of protruding carbide particles) has a relatively smooth etched surface revealing some individual carbide particles after being etched in 2% Nital, while the “sunken” matrix areas in the same figure have a very “rough” etched surface which consists of a fine internal and parallel striated structure that has clearly etched very much differently from the “raised” smooth matrix areas.

It may, therefore, be concluded that the raised matrix areas appear to be one phase whereas the sunken matrix areas are clearly another phase or even a multiphase (except for the carbide particles which are present in both types of areas). Consequently, there are apparently two types of matrix phases in alloy #6. Taking all of the above evidence of optical, SEM and TEM observations together, it was concluded that the smooth and raised matrix phase in figure 7.34 is most likely polygonal ferrite (marked with “PF”), whereas the striated and deeper etched one is likely to be acicular ferrite (marked with “AF”). This result was further validated with

thin foil samples in sections 8.3 and 8.4 in the next chapter. As can be seen in figure 7.34, the shadowing is also effective to reveal the smaller precipitates and grain boundaries (marked with "GB") by enhancing their presence.

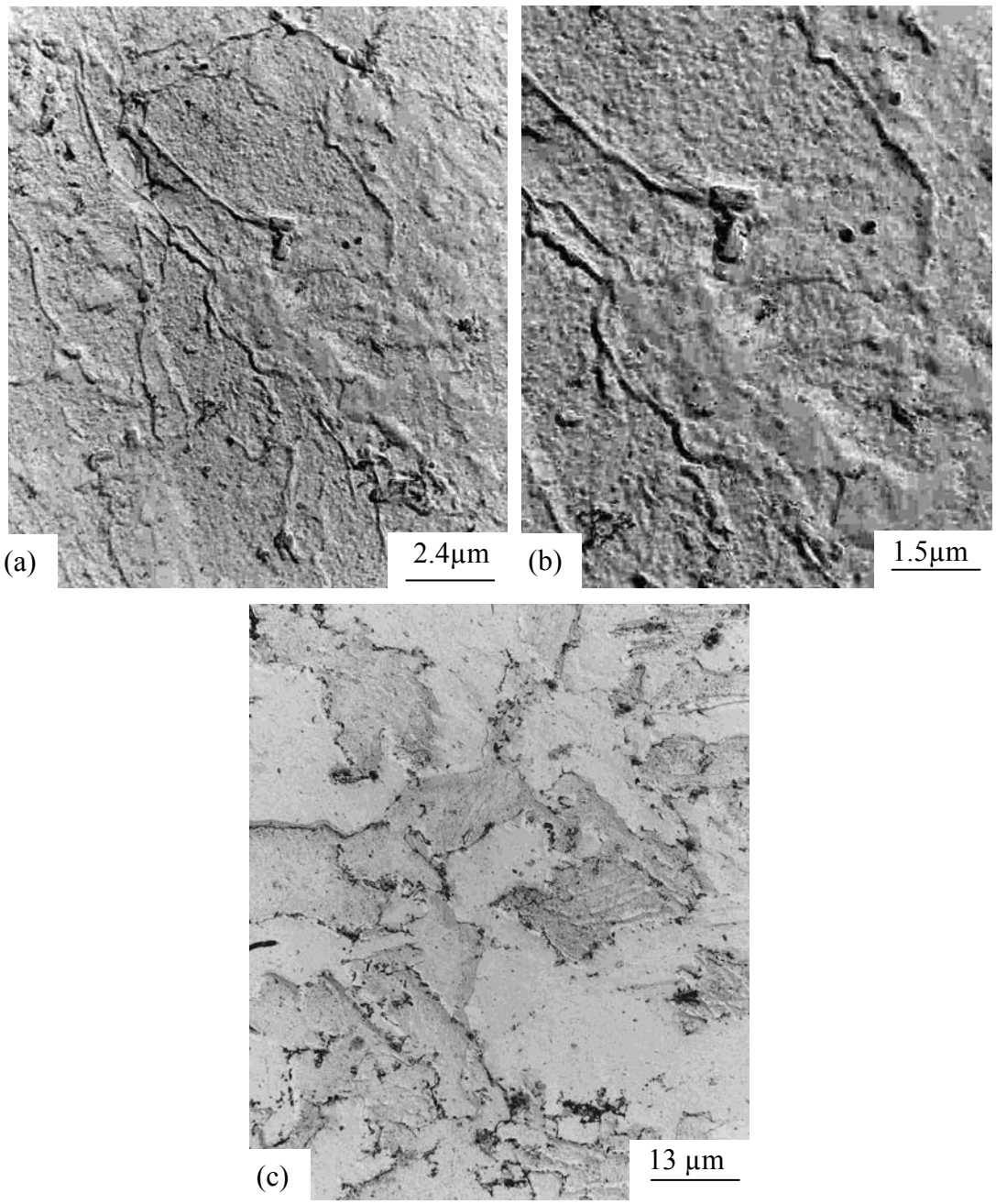

Figure 7.33 TEM micrographs of carbon extraction replicas without shadowing for the reference alloy #6 after hot rolling and rapid cooling at a rate of 39 ºCs^{-1}.

Summarising these results, it was concluded that the shadowing of extraction carbon replicas by applying Au-Pd shadowing at an angle to the etched surface, is an

improved technique to identify the matrix structures in these alloys as both acicular ferrite and polygonal ferrite can be clearly distinguished from each other. The microstructure of reference alloy #6 after hot rolling and rapid cooling at a rate of 39 $^{o}Cs^{-1}$ is, therefore, one of polygonal ferrite plus acicular ferrite with some individual smaller carbides in both these matrix phases.

By this technique, it was also confirmed that the microstructures of the experimental alloys #1 to #5 equally consisted of both polygonal ferrite and acicular ferrite (see figure 7.35) while no structure in the entire study was found with 100% acicular ferrite. The mixed microstructures of the five experimental alloys were, therefore, very similar to that found in the reference Mo-free alloy.

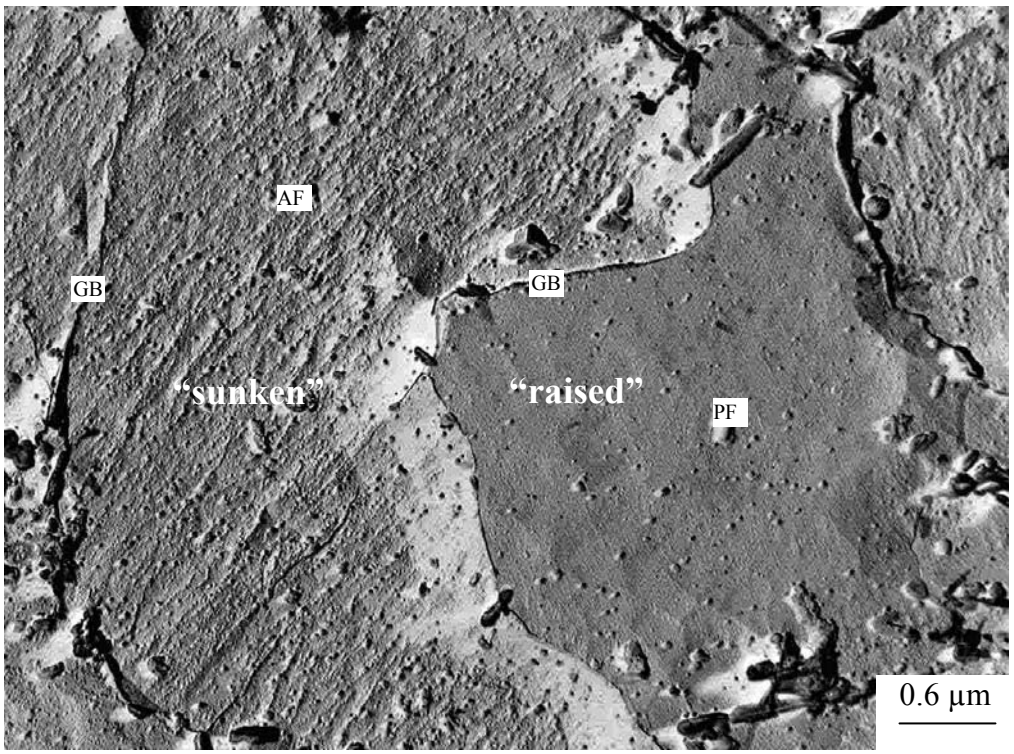

Figure 7.34 The TEM micrograph from a shadowed replica of the Mo-free alloy #6 after hot rolling and rapid cooling at a rate of 39 $^{o}Cs^{-1}$. (AF-acicular ferrite, PF-polygonal ferrite and, GB-grain boundary).

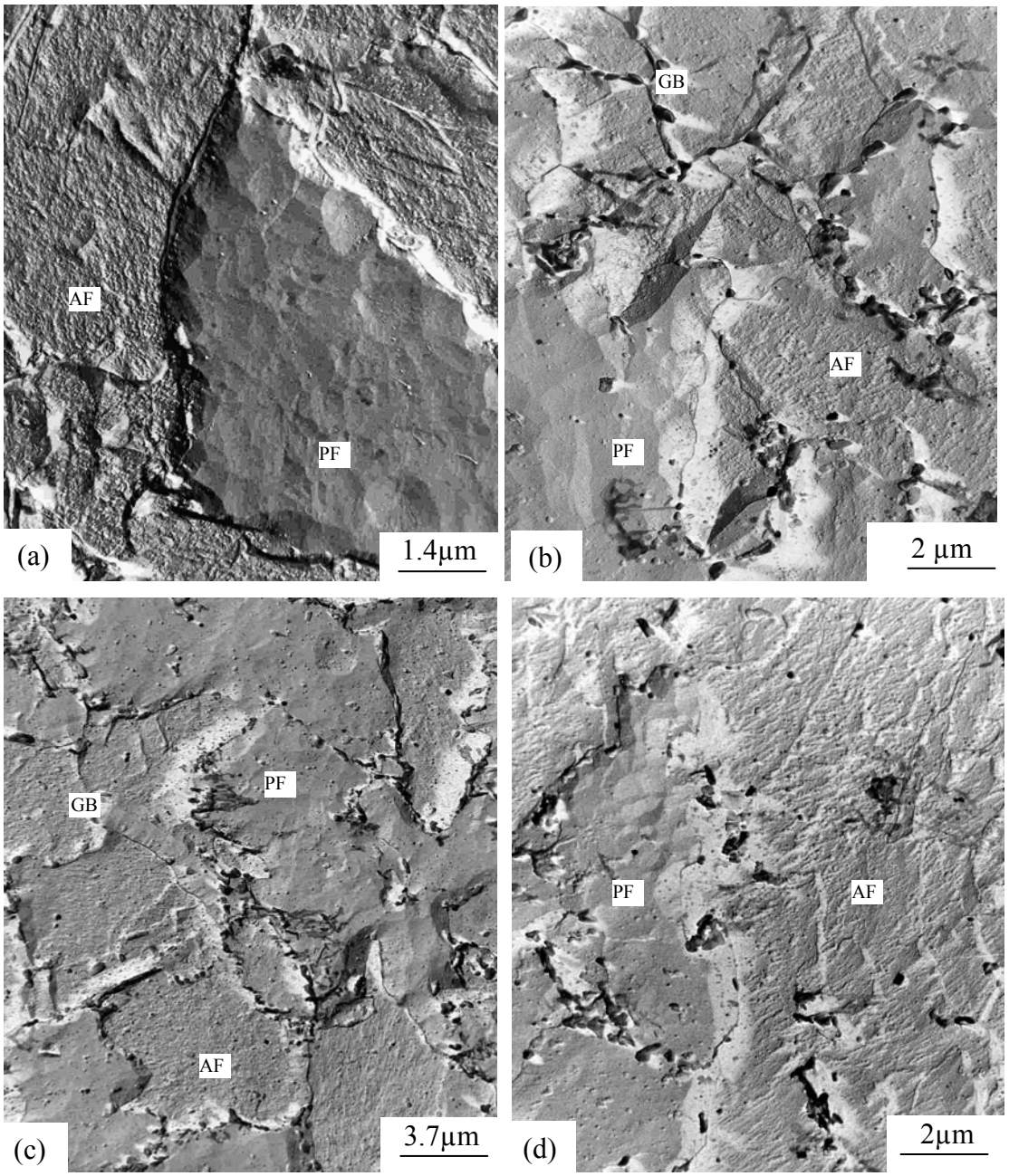

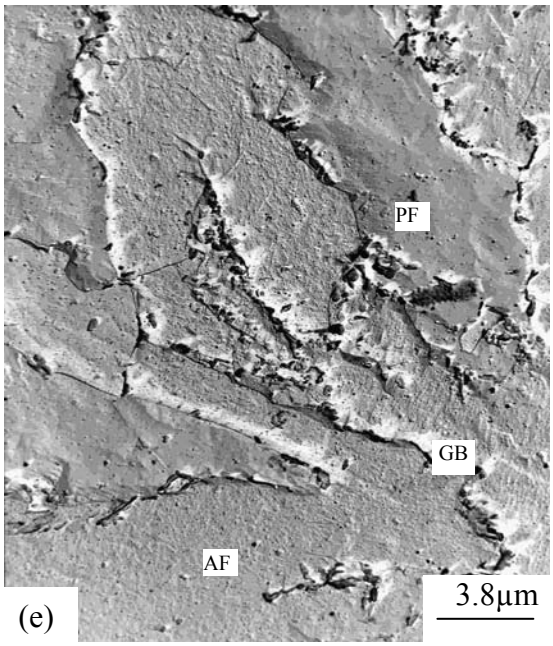

Figure 7.35 TEM micrographs from shadowed replicas of the as-hot rolled and rapidly cooled (at a rate of 47 ºCs^{-1}) experimental alloys (a) #1, (b) #2, (c) #3, (d) #4 and, (e) #5 (AF-acicular ferrite, PF- polygonal ferrite and, GB-grain boundary).